Desalination and Water Treatment
www.deswater.com
1944-3994/1944-3986 © 2012 Desalination Publications. All rights reserved
doi: 10/5004/dwt.2012.3009

Taylor & Francis
Taylor & Francis Group

42 (2012) 269–273
April

3D numerical simulation on mixing process in ducts of rotary pressure exchanger

Liu Yu*, Zhou Yi-Hui*, Bi Ming-Shu

School of Chemical Machinery, Dalian University of Technology, Dalian 116024, China
Tel. +86 411 3960 8115, +86 411 84986330; Fax: +86 411 3960 8115; emails: zhou-yihui@163.com, 286041250@qq.com

Received 2 June 2011; Accepted 16 October 2011

ABSTRACT

Since there is no physical barrier between the brine and seawater streams in the rotor ducts of rotary Pressure Exchanger (RPE), the degree of mixing between these streams has become an important criterion of the performance of RPE. In this paper, a 3D numerical simulation mode of a whole RPE is presented, followed by an illustration and discussion of the computational results to analyze the relationship between the rotation speed, flow rate and fluid mixing. It is demonstrated that under certain conditions, a stable liquid plug can be formed in RPE channels. It is clearly seen that movement of a liquid piston separates the fresh water and brine to prevent from over-mixing with each other. Moreover, the mixing in RPE was controlled by the operating conditions. It was found that the volume mixing ratio rises with increase of flow rate and decrease of rotation speed.

Keywords: Numerical simulation; Mixing; Rotary pressure exchanger; Liquid piston; SWRO; 3D numerical simulation; Volumetric efficiency

1. Introduction

RPE has become an indispensable component in reverse osmosis desalination systems because of its simple design, low operating costs, high stability and reliability and its closed to 100% energy recovery efficiency compared with another energy recover devices [1]. Instead of using a solid piston like other traditional work exchangers, the mixing in RPE was controlled by the design of the duct and operating conditions because there is no physical barrier between the brine and seawater in the rotor ducts. The concentration of fresh seawater at high pressure outward pipe should not be so increased because of effect on the reverse osmosis (2.5% salinity increase at high pressure outward pipe leading to the increase of operating pressure by 0.13 MPa [1]). So the degree of mixing between these streams has become an important criterion to reduce the cost of SWRO system desalination.

The numerical modeling literature on RPE is few due to its complexity. Wang Yue and Wang Shi-chang [2] simplified the three-dimensional mixing process to one dimension, and tried to introduce the mixing progress in the RPE's ducts, and the relationship between the velocity of the flow inlet and the degree of mixing was studied. However, this numerical simulation mode cannot accurately simulate the real operation conditions, as this model ignores the fact that liquid plug is only formed after several stroke cycles.

Zhou Yihui et al. [3] developed a 2D numerical simulation for RPE device to simulate the dynamic mixing process in the ducts. The transition process and conditions from initial mixing zone to the liquid piston were explained through 2D numerical simulation. Results of this computation illustrated the mixing progress and indicated that a stable liquid plug can be formed in the RPE channels.

*Corresponding authors.

2011 Qingdao International Desalination Conference Symposium on Desalination and Water Treatment Global Platform for Water Solutions, June 20–23, 2011 Qingdao, China

However, the 2D numerical simulation model in the previous studies cannot fully express the radial flow in the channels and is exclusively applicable to symmetric channels. This paper, designating a 3D numerical simulation mode of a RPE, investigates the mixing progress and the relationship between the rotation speed, flow rate and fluid mixing.

2. 3D numerical simulation on dynamics mixing in ducts

2.1. Geometry model

The structure of RPE is depicted in Fig. 1, including the brine endcover, the seawater endcover, sleeve and rotor. The rotor is 108 mm in diameter, 150 mm long with 12 holes parallel with each other.

A 3D simulation model based on the above structure is displayed in Fig. 2. At first, the fresh seawater fills up a chamber inside a rotating duct, then the rotor rotates, and the duct enters a seal zone where flow stops. The duct continues to rotate, when the duct is exposed to the incoming HP brine inlet, the fresh feed seawater is displaced and pressurized toward the membranes. At last, the rotor turns back and a new round of cycle starts again.

2.2. Governing equations and boundary conditions

2.2.1. Governing equations

The numerical simulation is carried out under cylindrical coordination. And the governing equations are [4]:

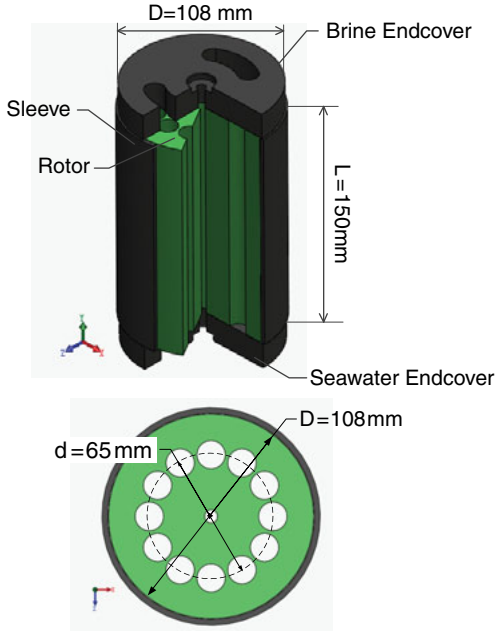

Fig. 1. Structure view of the rotary pressure exchanger.

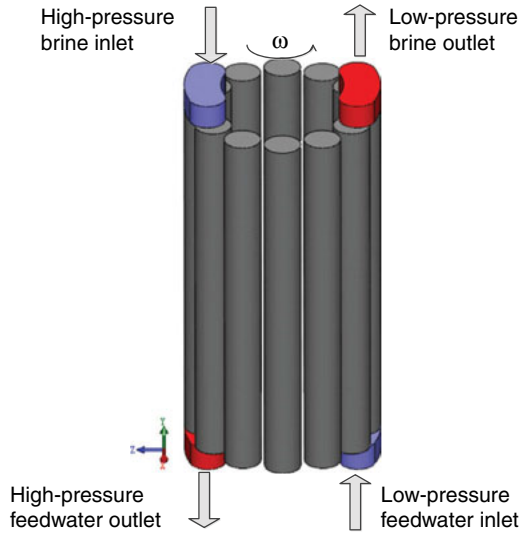

Fig. 2. Geometry model of 3D mixing simulation.

Continuity equation:

$$\frac{\partial \rho}{\partial t} + \nabla \cdot \left(\partial \vec{\rho} \right) = 0 \tag{1}$$

Momentum equation:

$$\frac{\partial}{\partial t}\left(\rho \vec{\upsilon}\right) + \nabla \cdot \left(\rho \vec{\upsilon}\vec{\upsilon}\right) = -\nabla P + \nabla \cdot \left(\bar{\bar{\tau}}\right) + \rho \vec{g} \tag{2}$$

Specifies equation:

$$\frac{\partial}{\partial t}\left(\rho Y_i\right) + \nabla \cdot \left(\rho \vec{\upsilon} Y_i\right) = -\nabla \cdot \vec{J}_i + R_i \tag{3}$$

In turbulent flows:

$$\vec{J}_i = -\left(\rho D_{i,m} + \frac{\mu_t}{Sc_t}\right)\nabla Y_i - D_{T,i}\frac{\nabla T}{T} \tag{4}$$

Turbulence model: the standard k– ε model

Turbulent kinetic energy:

$$\frac{\partial}{\partial t}\left(pk\right) + \frac{\partial}{\partial x_i}\left(pku_i\right) = \frac{\partial}{\partial x_i}\left[\left(\mu + \frac{\mu_t}{\sigma_k}\right)\frac{\partial k}{\partial x_i}\right] + G_k + \rho\varepsilon \tag{5}$$

Turbulent energy dissipation:

$$\frac{\partial}{\partial t}\left(\rho\varepsilon\right) + \frac{\partial}{\partial x_i}\left(\rho\varepsilon u_i\right) = \frac{\partial}{\partial x_j}\left[\left(\mu + \frac{\mu_t}{\sigma_\varepsilon}\right)\frac{\partial \varepsilon}{\partial x_j}\right] + C_{1\varepsilon}\frac{\varepsilon}{k}\left(G_k + C_{3\varepsilon}G_b\right) - C_{2\varepsilon}\rho\frac{\varepsilon^2}{k} \tag{6}$$

2.2.2. Boundary conditions

Non-slip boundary condition is used on the inner wall of the ducts. The standard wall function method is applied to simulate the flow state in the near-wall region. The mass-flow-inlet boundary condition is used on the high-pressure brine inlet, low-pressure feed water inlet and the pressure-outlet boundary condition is used on the high-pressure feed water outlet, low-pressure brine outlet. The rotor speed is given by cell zone conditions.

2.3. Grid generation and numerical method

The grid of the computation model is schematically displayed in Fig. 3(a).

The number of the grid is 196864, which is generation by unstructured tetrahedral mesh. Mesh density depends on the near-wall modeling strategy adopted for resolving the problem under turbulent flow conditions, displayed in Fig. 3(b).

In this paper, the numerical simulations are carried out using the FLUENT software, which is based on a control volume discretization method. The Runge-Kutta algorithm was employed to solve the linear equation set. Moreover, the SIMPLE pressure-based solver is selected.

3. Results and discussion

3.1. Mixing formation in the duct

First, at the initial conditions the ducts are filled with 1.8% fluid. The mixing process does not reached equilibrium till the steady mixing is formed. In addition, operating the RPE with unbalanced flows will cause the seawater feed contaminated by the brine reject. Therefore the high and low-pressure brine flows are always equal in the boundary conditions. Furthermore, in practice, flow rate and rotation speed are coupled, because the rotor is driven by the flow-inlet. However, in this paper in order to reduce influencing factors of mixing progress, flow rate and rotation speed are independent.

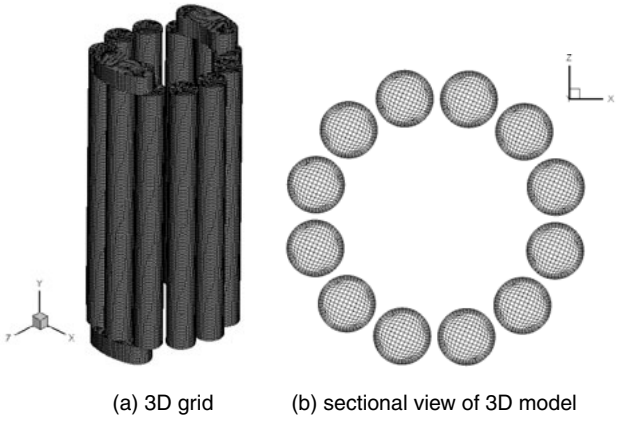

Fig. 3. Meshes of computational model. (a) 3D grid, (b) sectional view of 3D model.

Fig. 4(a)–(d) illustrate the species concentration on the ducts at the different time point from 0.2–1.4 s. The red area represents brine water whose concentration is 3.5%. The blue represents the fresh water whose concentration is 1.8%. The transition between the two colors is the mixing zone. As the time goes by, the length of the mixing section is increasing, and the mixing section is moving to the middle of the ducts. After the species concentration on the outlet face is constant, which means the steady fluid plug formed, the computation is completed. Table 1 shows the computation conditions.

The stabilized time of the liquid piston is a function of both stream velocity and the rotation speed. Larger inlet velocity or smaller rotation speed means less stabilized time for the device. In this geometry model, time for the process to reach steady mixing is 1–4.5 s.

3.2. Liquid piston in the ducts

Fig. 5(a) shows the concentration distribution in all the ducts of a rotor when the mixing is steady after 5.6 s. It could be clearly seen that the liquid piston formation in the ducts during rotation. Table 2 shows the computation condition.

Fig. 5(b) illustrates the concentration of the one duct at different positions of the rotor during one rotation period.

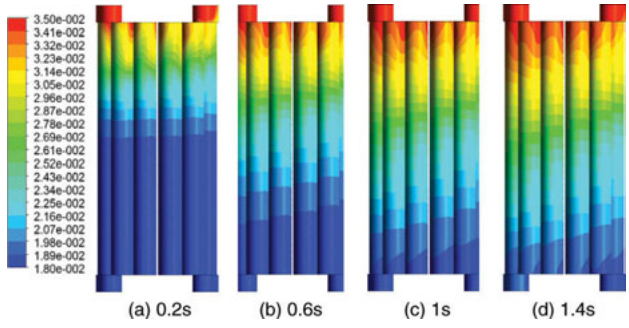

Fig. 4. The process of the steady mixing formed.

Table 1
Computation conditions for steady mixing formation

Rotor speed (r min^{-1})	Flow rate (m^3 s^{-1})	Flow velocity (m s^{-1})	Species concentration (%)	Steady time (s)
1200	0.0005	1.32	3.5–1.8	2.0

Table 2
Computation conditions for liquid piston in the ducts

Rotor speed (r min^{-1})	Flow rate (m^3 s^{-1})	Flow velocity (m s^{-1})	Species concentration (%)	Steady time (s)
1200	0.0007	1.85	3.5–1.8	2.0

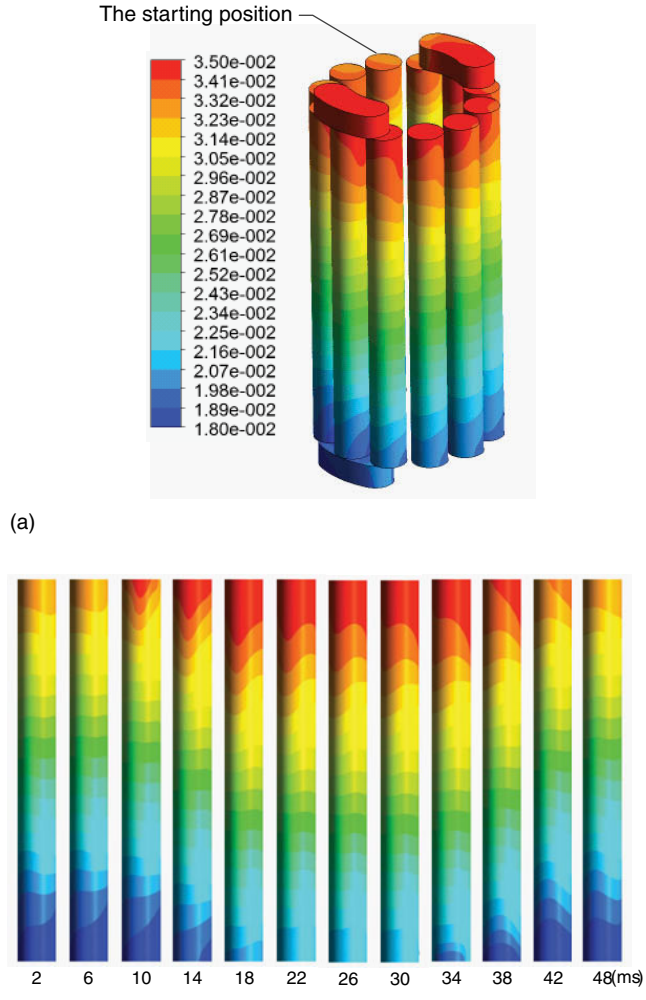

Fig. 5. Liquid piston in the ducts of rotor. (a) Structure view of concentration distribution in all the ducts of a rotor, (b) concentration of the one duct at different positions during one rotation period.

The rotation starts from seal zone and then the 3.5% NaCl high pressure brine flows into the duct. At the same time, the liquid piston is pressurized to move down to the end cover. The 1.8% NaCl is almost pushed out of the duct, and the flow-in length of high pressure fluid goes to its maximum. Then, after another seal area, the 1.8% NaCl enters the duct while the 3.5% NaCl is pushed out of the duct. It is clearly seen that movement of the liquid piston separates the fresh water and brine to prevent from over-mixing with each other.

3.3. Parameters affecting mixing rate

Many parameters affect the mixing rate, in which flow-in velocity and rotation speed are the most important ones. For this reason, these two parameters are specifically studied in this paper. Fig. 6 shows the relationship between flow inlet and volumetric mixing rate. Mixing rate [1] is calculated using the following Eq. (7). As the flow inlet increases, the volumetric mixing rate increases as well. It is because the turbulence intensity will increase with the velocity of the flow. However, process of the mass transfer is strengthened by the increased turbulence intensity.

$$\text{Volumetric mixing} = \frac{\text{HP}_{\text{out}}\ \text{salinity} - \text{LP}_{\text{in}}\ \text{salinity}}{\text{HP}_{\text{in}}\ \text{salinity} - \text{LP}_{\text{in}}\ \text{salinity}} \quad (7)$$

The relationship between rotation speed and the volumetric mixing is illustrated in Fig. 7. It is the computational results when inlet flow rate is 0.0005 m^3 s^{-1} and rotation speed varying from 600–1600 rpm.

As the rotation speed increases, the degree of mixing is decreased, which simply because the duration of exposure decreased. Furthermore, at the low rotation speed (less than 400 gpm), the RPE cannot form a stable position and the mixing occurs seriously. This is because the duration of exposure is so long that the flow inlet can pass almost the whole duct, and the species will be completely transferred from the brine water to

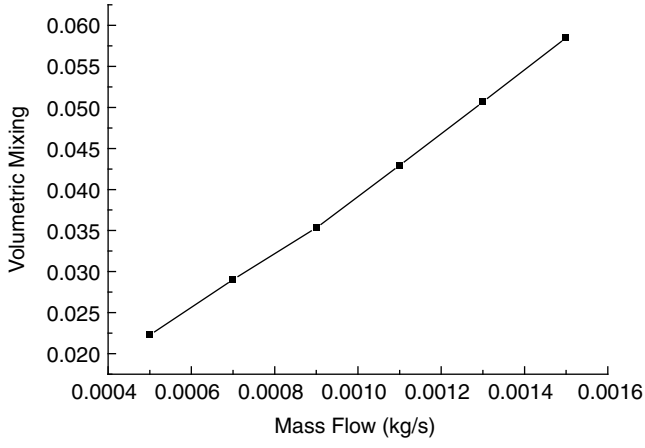

Fig. 6. Relationship between flow inlet and volumetric mixing rate.

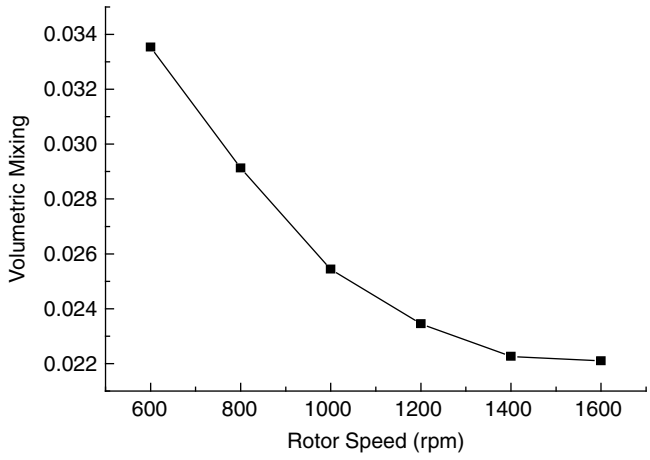

Fig. 7. Relationship between rotation speed and volumetric mixing.

fresh water which leads to the RPE cannot conform to the stable liquid plug between the brine water and the feed fresh water.

It can be seen from the ranges of volumetric mixing rate shown in Figs. 6 and 7 that inlet flow rate is the main factor affecting the volumetric mixing rate because it causes more dramatic increasing of volumetric rate than that of rotor speed. In addition, their effective trend is opposite which means the effectiveness will cancel with each other finally.

4. Conclusions

The 3D dynamic mixing model is set up according to RPE. The mixing process is simulated to get the steady mixing formation time, the mixing formation process and their effective parameters. Simulation results illustrate that during rotation the mixing zone reciprocally moves in the duct. Both the flow inlet and the rotation speed have effects on volumetric mixing of which the flow rate is the more important one. However, their effectiveness are opposite and will cancel with each other finally.

References

[1] R.L. Stover, Development of a fourth generation energy recovery device-A 'CTO's Notebook', Desalination, 165 (2004) 313–321.
[2] W. Yue and W. Shi-chang, Mixing behavior of feed and concentration in SWRO energy recovery cylinder and its computer simulation, Membr. Sci. Technol., 25(6) (2005) 36–39.
[3] Z. Yihui, D. Xinwei, et al., Numerical simulation on a dynamic mixing process in ducts of a rotary pressure exchanger for SWRO, Desalin. Water Treat., 1 (2009) 107–113.
[4] ERI Energy Recovery Inc., (2008). Installation, operation & maintenance manual 65-series pressure exchanger energy recovery devices ERI®DOCUMENT NUMBER 80019-01 REVISION.